A MATHEMATICAL MODEL FOR THE TRANSPORT OF PACLITAXEL (TAXOL) ACROSS THE BLOOD-BRAIN BARRIER

S. Bandara[1,*], M. Diehl[2] and G. Fricker[1]

[1]Institute of Pharmacy and Molecular Biotechnology, University of Heidelberg, Heidelberg, Germany.
[2]Electrical Engineering Department (ESAT), Kathdieke Universiteit Leuven, Leuven, Belgium.

Abstract: Paclitaxel (Taxol) from *Taxus brevifolia* is an antimitotic drug that is successfully used in the fight against many different types of cancers. However, exclusion of paclitaxel from the central nervous system by the blood-brain barrier is a major obstacle for paclitaxel-based treatment of glioma. Here, we propose a mathematical model for the transport of paclitaxel across the blood-brain barrier, based on ordinary differential equations, which considers (1) passive diffusion across the luminal and the abluminal membrane of brain capillaries, (2) luminal blood-binding and binding to microtubules within the brain capillary endothelial cells, and (3) active transport of paclitaxel from the endothelial cells to the vascular lumen by p-glycoprotein. With experimental data published previously, we show that the parameters of this model can be estimated with a simple experimental setup. The model presented here might support the rational development of targeting strategies *in silico* for efficiently delivering drugs across the blood-brain barrier.

Keywords: blood-brain barrier; drug transport; paclitaxel; parameter estimation.

*Correspondence to:
Mr S. Bandara, Department of Chemical and Systems Biology, Clark Center W200, 318 Campus Drive, Stanford University, Stanford CA 94305, USA.
E-mail: sbandara@stanford.edu

DOI: 10.1205/cherd06238

0263–8762/07/
$30.00 + 0.00

Chemical Engineering Research and Design

Trans IChemE,
Part A, July 2007

© 2007 Institution of Chemical Engineers

INTRODUCTION

The blood-brain barrier (BBB) prevents a variety of chemical compounds from entering the central nervous system (CNS) from blood via the wall of brain capillaries. The wall of a brain capillary is formed by endothelial cells which are tightly attached to each other, thus preventing paracellular diffusion (Dermietzel, 1975). However, the BBB also involves an active process which is mediated by the molecular transport protein p-glycoprotein (p-gp). This protein is localized in the luminal membrane of endothelial cells (Seetharaman *et al.*, 1998). With its broad substrate specificity, p-gp rapidly exports a variety of compounds to the vascular lumen—back to the blood. Thereby, the BBB also effectively prevents transcellular diffusion from blood to the CNS.

P-gp has an apparent molecular weight of 170 kD (Juliano and Ling, 1976) and is a member of the superfamily of ATP-binding cassette transporters (ABC-Transporters). P-gp-mediated efflux is energy-dependent, and is driven by the hydrolysis of ATP which ubiquitously serves as a source of energy within living cells. For p-gp, there is no known major substrate as ones are known for most other enzymes. Quite the contrary, p-gp does transport a variety of chemical compounds, and even several distinct sites on p-gp are considered to bind different families of substrate (Martin *et al.*, 2000). As p-gp is found in many higher organisms including fish, birds, and mammals, we might conclude that during evolution, p-gp has proven to be valuable in protecting the CNS against toxic metabolites and xenobiotics. With the early beginnings of pharmacology, however, the human brain became a volitional target of xenobiotics. Today, drugs against brain diseases like depression, insomnia, epilepsy, Parkinson's and Alzheimer's disease, schizophrenia, and many others generate revenues of several billion USD (Maggon, 2005). From this it is clear, that in many cases, the BBB is a major impediment to promising drug candidates.

Glioblastoma multiforme (GBM) are high-grade tumours of the brain that are derived from glial cells, and that have poor prognostic outcome. With an annual incidence of four to five cases per 100 000 persons, and with short overall survival, GBM clearly is an orphan disease (Steiner *et al.*, 1998). Therefore, novel therapeutic approaches based on known drugs need to be developed. Paclitaxel (Taxol) from *Taxus brevifolia*, the pacific yew tree, is successfully used in the treatment of

many tumours (Rowinsky, 1997). Paclitaxel binds to microtubules which assemble from the monomeric protein tubulin and disassemble into tubulin monomers in a controlled equilibrium. By binding to microtubules, paclitaxel strongly perturbs this equilibrium in that it hyper-stabilizes the tubular polymeric form (Caplow *et al.*, 1994). During cell division, microtubules are needed to mechanically segregate the copies of chromosomes from each other. As many tumours are more proliferative than most normal tissues, and cell cycle control is damaged, the cytotoxic action of paclitaxel affects those neoplastic cells more strongly.

For brain tumours, however, the therapeutic benefit of paclitaxel is low (Glantz *et al.*, 1999). Interestingly, coadministration of paclitaxel and a p-gp inhibitor, valspodar, significantly reduced the volume of xenograft GBM tumours in the brain of mice, compared to treatment with paclitaxel alone (Fellner *et al.*, 2002). P-gp was first discovered not at the BBB but in chemoresistant tumours (Juliano and Ling, 1976), and today, it seems to be clear that overexpression of p-gp and of related ABC transporters is a major mechanism of chemoresistance in tumours. For that reason, another name of p-gp is multidrug resistance protein (MDR). Poor results from the treatment of brain tumours using paclitaxel can, however, clearly be attributed to the BBB, rather than to chemoresistance, as resistance would be innate, and as intravenous injection of paclitaxel yields remarkably low concentrations in the CNS (Heimans *et al.*, 1994).

An experiment using isolated brain capillaries from rats (Fellner *et al.*, 2002) provided evidence that p-gp indeed is responsible for reduced uptake of paclitaxel into the brain. Here, we propose a mathematical model for the molecular transport of paclitaxel across the BBB, based on ordinary differential equations (ODEs), and present parameter estimates obtained by least square-fitting this model to time-course data acquired in that study (Fellner *et al.*, 2002), using the optimization software MUSCOD-II (Leineweber *et al.*, 2003) which implements a multiple shooting approach with Gauss–Newton Hessian (Diehl, 2002), as introduced by Bock (1987).

METHODS

The model was implemented as C code within the MUSCOD-II framework. The radii $r_L = 1.56 \pm 0.27$ μm and $r_E = 4.24 \pm 0.28$ μm were measured each at $n = 20$ different spots of a brain capillary using the ImageJ software (Rasband, 1997–2006), version 1.33u.

RESULTS

Experimental Findings

For their experiment, Fellner *et al.* (2002) isolated brain capillaries from rats, incubated them in Krebs-Henseleit buffer (KHB) with 1 μM BODIPY Fl-paclitaxel, which is a fluorescent derivative of paclitaxel, and took digital images of the capillaries at various time points, using fluorescence microscopy (see Fellner *et al.*, 2002 for experimental details). Both the endothelial and the luminal fluorescence intensity were quantified in arbitrary units (AU) by digital analysis of the images taken 15, 20, 30, 45, and 60 min after 1 μM BODIPY Fl-paclitaxel in KHB was added to the capillaries. After 30 min, equilibrium was reached in both compartments [Figure 1(A)], with the fluorescence intensity in the lumen (~150 AU) reaching a three times higher level than in the endothelial cells (~50 AU). The experiment was repeated with both 1 μM BODIPY Fl-paclitaxel and 1 mM sodium cyanide (NaCN) in KHB. The cyanide anion (CN^-) blocks the respiratory chain by inhibiting cytochrome oxidase in the mitochondrial membrane, which results in the complete breakdown of all energy-dependent processes (Ball and Cooper, 1952). After equilibrium was reached without active transport, the endothelial concentration was the same (~50 AU), whereas the luminal concentration reached ~65 AU, only [Figure 1(B)]. With and without NaCN, the surrounding medium was dark, clearly indicating that both the luminal and the endothelial concentration of BODIPY Fl-paclitaxel were much higher than 1 μM.

Development of the Model

Fluorescence was quantified in two compartments: in the lumen and in the endothelial cells of the brain capillaries. For the free concentration of BODIPY Fl-paclitaxel in these compartments, two differential states, $c_{f,L}$ and $c_{f,E}$, were defined. The concentration in the surrounding medium, c_M, was considered to be constant, because its volume was much larger than the volume of the capillaries. In the human brain, the total length of all capillaries is estimated to be $l = 600$ km. In our model, however, we consider the cross-section of a single tube-like capillary. The geometry of this cross-section is given by the luminal radius r_L and the endothelial outer radius r_E, as the luminal volume V_L, the endothelial volume V_E, the surface area between lumen and endothelia A_{LE}, and the outer surface area of the capillary A_{EM} all can be derived from these parameters:

$$\begin{aligned} V_L &= \pi r_L^2 l \\ V_E &= \pi (r_E^2 - r_L^2) l \\ A_{LE} &= 2\pi r_L l \\ A_{EM} &= 2\pi r_E l \end{aligned} \tag{1}$$

Capillaries of the periphery are fenestrated by pores between endothelial cells, allowing molecules to equilibrate freely between blood and surrounding tissues by paracellular diffusion. In the CNS, however, capillaries are not fenestrated, and endothelial cells establish tight junctions that prevent molecules from paracellular diffusion (Dermietzel, 1975). In the experiment, the integrity of each capillary was confirmed after isolation, using the non-permeating fluorescent compound FITC-dextran which did not cause detectable luminal fluorescence in a period of incubation of more than 60 min. Therefore, transport by diffusion occurred across membranes only, and was modelled between lumen and endothelial cells, and between endothelial cells and surrounding medium, but not between lumen and medium:

$$J_{LE} = D_{LE} A_{LE} (c_{f,L} - c_{f,E}) \tag{2}$$

$$J_{EM} = D_{EM} A_{EM} (c_{f,E} - c_M) \tag{3}$$

Diffusion linearly depends on the gradient of concentration and on the area of the boundary layer between the compartments involved. As corrugation of the membranes, unequal lipid composition in the membranes, or additional barriers affect the speed of diffusion, a different diffusion coefficient for the

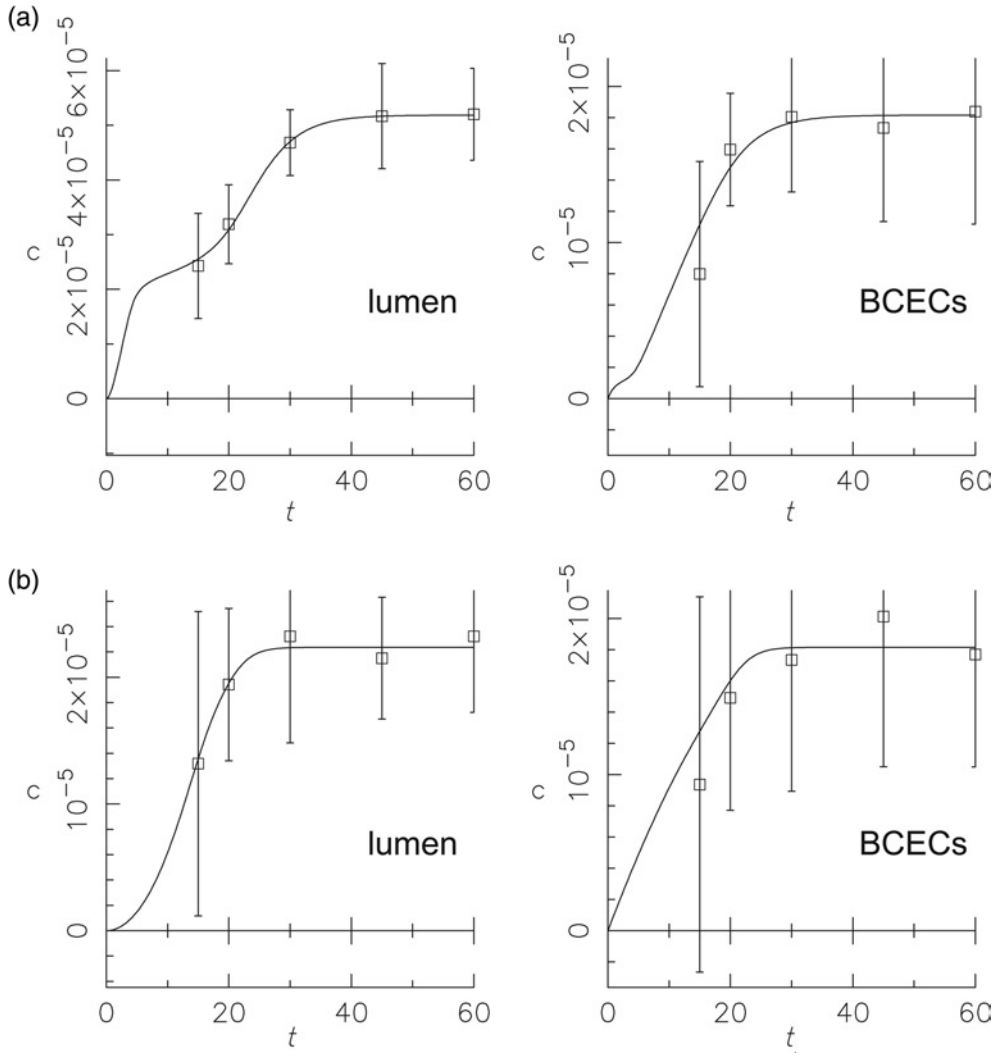


Figure 1. Parameter estimation. Concentration of BODIPY Fl-paclitaxel in the lumen and in the brain capillary endothelial cells, as measured (open squares) and as reproduced by the model (continuous lines), for the capillaries incubated in (a) 1 μM BODIPY Fl-paclitaxel alone or (b) 1 μM BODIPY Fl-paclitaxel and 1 mM NaCN. Arbitrary units were converted to molarities using the parameter estimate α. Error bars represent the standard deviation in the original data. The incubation time t is given in minutes, and the concentration c in moles per litre.

transport across each membrane, D_{LE} or D_{EM}, respectively, was defined as a model parameter. P-gp reduces the uptake of paclitaxel in many chemoresistant tumours, and also is expressed in high levels in the endothelial cells of the BBB. The p-gp inhibitor valspodar strongly enhanced the effect of paclitaxel on xenograft GBM tumours in the brain of mice (Fellner *et al.*, 2002). As paclitaxel is excluded from the CNS by active transport, p-gp is commonly considered to be the major transporter protein of paclitaxel at the BBB. Immunostaining showed that p-gp is predominantly localized in the luminal membrane of the brain capillary endothelial cells (BCECs), and that the amount of p-gp in the outer, abluminal membrane of the capillary is negligible (Seetharaman *et al.*, 1998). For that reason, active transport of BODIPY Fl-paclitaxel was introduced to the model only from endothelia to lumen. Previously, standard transporter kinetics was successfully applied in a mathematical model for p-gp-mediated resistance of cultured tumor cells against paclitaxel (Jang *et al.*, 2001). According to these kinetics, transport from endothelial cells to the vascular lumen is concentration dependent, saturable, and can be described by

$$J_{pgp} = \frac{J_{max} c_{f,E}}{K_M + c_{f,E}} \tag{4}$$

The molecular mode of action of paclitaxel is to hyper-stabilize microtubules by binding to them, thus blocking the mitotic apparatus of dividing cells (Caplow *et al.*, 1994). However, microtubules are also integral parts of the cytoskeleton, serving various functions throughout the cell. From that, it is clear why tubulin is ubiquitously expressed in large amounts, also in BCECs, and therefore, intracellular binding of BODIPY Fl-paclitaxel must be considered by our model. As there is presumably no active transport of BODIPY Fl-paclitaxel across the outer membrane, intracellular binding also explains why endothelial fluorescence was high, whereas the surrounding medium was dark. As many other drugs, paclitaxel binds to various structures within the blood. Theses are part of blood cells like erythrocytes and platelets, and sites on plasma proteins like albumin and alpha acid glycoprotein

(Henningsson *et al.*, 2001). Because in the experiment, it was confirmed that the capillaries were intact after isolation and washing, our model must consider luminal binding.

For simplification, for each of the two compartments, one differential state representing the concentration of bound BODIPY Fl-paclitaxel was introduced to the model, $c_{b,L}$ and $c_{b,E}$, together with parameters for the maximum binding capacity ($B_{max,L}$ and $B_{max,E}$) and for the rates of association ($k_{a,L}$ and $k_{a,E}$) and of dissociation ($k_{d,L}$, and $k_{d,E}$). For both compartments, the change of bound BODIPY Fl-paclitaxel has the form of

$$\frac{dc_b}{dt} = k_a c_f (B_{max} - c_b) - k_d c_b \tag{5}$$

As KHB was free of BSA and of any other molecule that would bind BODIPY Fl-paclitaxel, no binding in KHB was modelled. Rather, as mentioned above, the concentration in surrounding medium was considered to be constant, $c_M = 1\ \mu M$.

Taken together, the model presented here considers passive diffusion between medium and endothelial cells and between endothelial cells and lumen across membranes, concentration-dependent and saturable active transport from endothelial cells to the lumen mediated by p-glycoprotein, and intracellular and luminal binding of BODIPY Fl-paclitaxel to saturable structures. It is based on four differential states ($c_{f,L}$, $c_{f,E}$, $c_{b,L}$ and $c_{b,E}$, see Table 1) and 12 parameters (r_L, r_E, D_{LE}, D_{EM}, J_{max}, K_M, $B_{max,L}$, $k_{a,L}$, $k_{d,L}$, $B_{max,E}$, $k_{a,E}$, and $k_{d,E}$), and is given by the following system of ODEs:

$$\frac{dc_{f,L}}{dt} = \frac{1}{V_L}\left(A_{LE}D_{LE}(c_{f,E} - c_{f,L}) + \frac{J_{max}c_{f,E}}{K_M + c_{f,E}}I\right) - \frac{dc_{b,L}}{dt} \tag{6}$$

$$\frac{dc_{f,E}}{dt} = \frac{1}{V_E}\left(A_{LE}D_{LE}(c_{f,L} - c_{f,E}) + A_{EM}D_{EM}(c_M - c_{f,E}) - \frac{J_{max}c_{f,E}}{K_M + c_{f,E}}I\right) - \frac{dc_{b,E}}{dt} \tag{7}$$

$$\frac{dc_{b,L}}{dt} = k_{a,L}c_{f,L}(B_{max,L} - c_{b,L}) - k_{d,L}c_{b,L} \tag{8}$$

$$\frac{dc_{b,E}}{dt} = k_{a,E}c_{f,E}(B_{max,E} - c_{b,E}) - k_{d,E}c_{b,E} \tag{9}$$

Table 1. Differential states of the model. The concentrations of free and bound paclitaxel in the lumen and in the endothelial cells of brain capillaries were considered in this work, since parameters were estimated from experiments with isolated capillaries. Diffusion across the abluminal membrane gives access to the brain.

$c_L = c_{f,L} + c_{b,L}$	Total concentration of paclitaxel in the lumen of a brain capillary.
$c_{f,L}$	Concentration of unbound paclitaxel in the lumen.
$c_{b,L}$	Concentration of paclitaxel bound to blood in a brain capillary.
$c_E = c_{f,E} + c_{b,E}$	Total concentration of paclitaxel in brain capillary endothelial cells.
$c_{f,E}$	Concentration of unbound paclitaxel in endothelial cells.
$c_{b,E}$	Concentration of bound paclitaxel in endothelial cells.
c_B	Total concentration of paclitaxel in the brain (cerebro-spinal fluid, glia and neuronal cells).
$c_{f,B} = c_M$	Concentration of free paclitaxel in the cerebro-spinal fluid. In the experiment for parameter estimation, this differential state corresponded to the concentration of paclitaxel in the medium, which was constant.

Substitution in equations (6) and (7) using (1) reduces this ODE to a model observing the cross-section of a brain capillary:

$$\frac{dc_{f,L}}{dt} = \frac{2D_{LE}}{r_L}(c_{f,E} - c_{f,L}) + \frac{c_{f,E}}{K_M + c_{f,E}}\frac{J_{max}}{\pi r_L^2} - \frac{dc_{b,L}}{dt} \tag{10}$$

$$\frac{dc_{f,E}}{dt} = \frac{2r_L D_{LE}}{r_E^2 - r_L^2}(c_{f,L} - c_{f,E}) + \frac{2r_E D_{EM}}{r_E^2 - r_L^2}(c_M - c_{f,E}) - \frac{c_{f,E}}{K_M + c_{f,E}}\frac{J_{max}}{\pi(r_E^2 - r_L^2)} - \frac{dc_{b,E}}{dt} \tag{11}$$

Parameter Estimation

In their experiment, Fellner *et al.* (2002) measured the fluorescence intensity in the luminal and the endothelial compartment of brain capillaries at various time points after 1 μM BODIPY Fl-paclitaxel in KHB was added. As no fluorescence was detectable before the addition of this compound, the initial value of each state is zero. Assuming that fluorescence linearly depends on concentration over a wide range, a calibration factor, α, was introduced as another free parameter, because concentrations were determined in arbitrary units. The measured fluorescence was emitted both by free and by bound BODIPY Fl-paclitaxel. Therefore, $\alpha c_L = \alpha\ (c_{f,L} + c_{b,L})$ was fit to the data obtained for the vascular lumen, and $\alpha c_E = \alpha\ (c_{f,E} + c_{b,E})$ was fit to the data obtained for the endothelial cells, by finding the least sum of squares of the distances between data and model using an implementation of the multiple shooting Gauss–Newton algorithm (Bock, 1987; Leineweber *et al.*, 2003).

The multiple shooting method for parameter estimation, as developed by Bock (1987), has emerged to be the method of choice for parameter estimation of nonlinear dynamic system models. Like any other Gauss–Newton type algorithm, it is based on successive system linearizations and solutions of linearized least squares problems to obtain the next iterate. In contrast to a straightforward approach that just uses an initial value problem solver together with the Gauss–Newton method, the multiple shooting method choses different points for the system linearizations and does not rely on a system simulation along the full time horizon, with possibly wrong parameters. This is a crucial advantage when models are strongly nonlinear or unstable. Its main idea is to divide the full time horizon of interest (i.e., where the measurements are taken) into a number of subintervals, and to solve initial value problems on these subintervals independently, with artificial initial values. The linearization of these independent initial value problems is used within each Gauss–Newton iteration, which does simultaneously solve for the linearized continuity conditions as well as the least squares minimization. Only at the end of these so called 'generalized Gauss–Newton' iterations the state trajectory is continuous, and thus biologically meaningful. During the optimization, however, the possibility to violate temporarily the continuity conditions allows to better treat nonlinear and unstable system models, and is even able to solve parameter estimation problems for chaotic system models (Kallrath *et al.*, 1993).

This was done simultaneously for time series acquired with active transport and without active transport (NaCN added). All parameters were free except for the radii r_L and r_E which were fixed to $r_L = 1.56\ \mu m$ and $r_E = 4.24\ \mu m$, which

reduced the number of free parameters from 13 to 11. For the data used in this study, equilibration between bound and unbound BODIPY Fl-paclitaxel was rather immediate than time-dependent in both the vascular lumen and the endothelial cells, in the time-scale of active transport and diffusion. Therefore, we set out to further reduce the model by merging the bound and the unbound state in each compartment, and defined the total concentration in the lumen c_L and the total concentration in the endothelial cells c_E as the only differential states of the simplified model:

$$\frac{dc_L}{dt} = \frac{2D_{LE}}{r_L}(c_{f,E} - c_{f,L}) + \frac{c_{f,E}}{K_M + c_{f,E}}\frac{J_{max}}{\pi r_L^2} \quad (12)$$

$$\frac{dc_E}{dt} = \frac{2r_L D_{LE}}{r_E^2 - r_L^2}(c_{f,L} - c_{f,E}) + \frac{2r_E D_{EM}}{r_E^2 - r_L^2}(c_M - c_{f,E}) - \frac{c_{f,E}}{K_M + c_{f,E}}\frac{J_{max}}{\pi(r_E^2 - r_L^2)} \quad (13)$$

The free concentration of BODIPY Fl-paclitaxel in the lumen $c_{f,L}$ and in the endothelial cells $c_{f,E}$ was calculated as a function of c_L or c_E, respectively, as immediate equilibration was assumed. In equilibrium, the total concentration is

$$c = c_f + c_b = c_f + \frac{B_{max}c_f}{K_D + c_f} \Leftrightarrow \times c_f^2 + (K_D + B_{max} - c)\cdot c_f - c\cdot K_D = 0 \quad (14)$$

Thus, the free concentration c_f indeed is a function of the total concentration c, and is given by

$$c_f(c) = -\frac{p}{2} + \sqrt{\frac{p^2}{4} + q}, \quad \text{with} \quad p = K_D + B_{max} - c \quad \text{and} \quad q = c\cdot K_D \quad (15)$$

By assuming equilibrium, the model took up two new parameters, $K_{D,L}$ and $K_{D,E}$, in exchange for the four rate constants for association and dissociation dropping out, thus reducing the number of free parameters from 11 to 9, with

$$k_A\cdot c_f\cdot(B_{max} - c_b) = k_D\cdot c_b \Leftrightarrow \frac{k_D}{k_A} = \frac{c_f\cdot(B_{max} - c_b)}{c_b} = K_D \quad (16)$$

Furthermore, the number of differential states dropped from 4 to 2. For this simplified model being fit simultaneously to both time series, with and without active transport, the Gauss–Newton algorithm readily achieved convergence, with the parameter estimates shown in Table 2.

Table 2. Parameter estimates for the transport of BODIPY Fl-paclitaxel across the BBB. The parameters r_L and r_E were fixed to values obtained by digital image analysis. All other parameters were estimated using the optimization software MUSCOD-II for fitting the model to the experimental data published by Fellner *et al.* (2002).

Parameter	Estimate
D_{LE}	34.8 ± 131.8 μm min^{-1}
r_L (fix)	1.56 ± 0.27 μm
K_M	1.50 ± 3.16 μM
J_{max}	2.42 ± 16.23 pmol min^{-1} dm^{-1}
r_E (fix)	4.24 ± 0.28 μm
D_{EM}	1.89 ± 5.26 μm min^{-1}
α	2.88 ± 8.03 AU μM^{-1}
$B_{max,L}$	22.4 ± 66.0 μM
$K_{D,L}$	50.6 ± 78.1 nM
$B_{max,E}$	17.9 ± 53.3 μM
$K_{D,E}$	45.9 ± 34.8 nM

DISCUSSION

Paclitaxel from *Taxus brevifolia* is successfully applied in the treatment of many tumours (Rowinsky, 1997). However, the treatment of brain tumours fails because the BBB prevents the entry of paclitaxel into the CNS (Heimans *et al.*, 1994). Here, we present a quantitative model based on ODEs that describes this process of exclusion, which comprises diffusion across both the luminal and the abluminal membrane of brain capillaries, binding in the lumen and in the endothelial cells, and active transport of free drug by p-gp from the endothelial cells to the lumen.

Currently, p-gp seems to be the major transporter at the BBB, preventing entry of paclitaxel into the brain, as the p-gp inhibitor valspodar significantly increases the effects of paclitaxel in the CNS (Fellner *et al.*, 2002). For reasons of topology, insertion of ABC transporters into the abluminal, outer membrane of brain capillaries would lead to substrate delivery to the brain. This explains why endothelial cells of the BBB are polarized, e.g., why both p-gp (Seetharaman *et al.*, 1998) and BMDP (Eisenblatter *et al.*, 2003) are found in the luminal membrane, whereas abluminal localization is negligible. Therefore, the model considers active transport from the endothelial cells to the vascular lumen, only.

In the experiments done by Fellner *et al.* (2002), isolated brain capillaries from rats were incubated with 1 μM BODIPY Fl-paclitaxel, and the fluorescence intensity both in the endothelial cells and in the lumen were measured at several time points after addition of this compound [Figure 1(a)]. Parameter estimation with the initial model which considered binding as a time-dependent process, indicated that binding is rather immediate compared to transport. The output of the model illustrates how BODIPY Fl-paclitaxel was captured by the endothelial cells and the lumen, before the free concentration rose to a level that led to considerable net transport across the luminal membrane by p-gp over a control experiment, in which active transport was inhibited by 1 mM NaCN [Figure 1(b)].

As a major shortcoming of this work, instead of non-fluorescent paclitaxel, a fluorescent conjugate with the BODIPY-Fl moiety had to be used to track concentrations. This is important in that for structurally modified compounds, different rates of diffusion and different affinity to binders like microtubules and p-gp must be expected. Figure 2 shows the chemical structure of both paclitaxel and its fluorescent derivative BODIPY Fl-paclitaxel. As BODIPY Fl-paclitaxel is commonly used for producing fluorescent microtubules in vitro (Melan, 1998), it is clear that the fluorescent moiety does not prevent binding to polymerized tubulin. However, its use in cellular systems like isolated brain capillaries for quantitative studies is discouraged, presumably because the BODIPY-Fl moiety mediates binding to other cellular structures. Indeed, control experiments revealed a staining pattern that was atypical of microtubules (not shown).

We propose this model for understanding the transport of drugs across the blood-brain barrier quantitatively, which is controlled by diffusion, active transport, and binding. Where

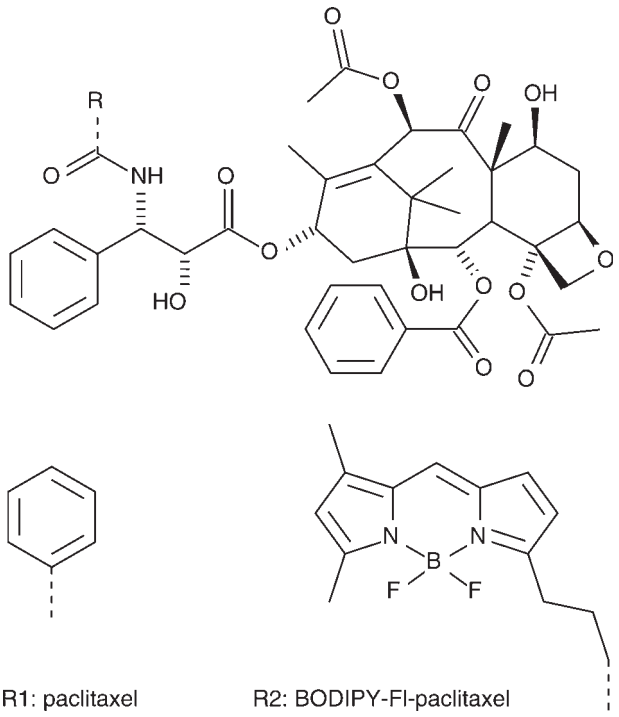


Figure 2. Chemical structure of paclitaxel and its fluorescent derivative BODIPY Fl-paclitaxel.

appropriate fluorescent derivatives of a drug are available, effects from membrane permeability, active transport and binding can be dissected by incubating isolated brain capillaries in the fluorescent compound and measuring the fluorescence in the lumen and in the endothelial cells at different time points as done by Fellner *et al.* (2002), and estimating the parameters of the model with numerical methods as presented here. Since variation in this assay is high, it is advisable to use varying concentrations of the fluorescent drug in the medium, and to observe washouts by replacing the medium with empty buffer, in order to obtain better parameter estimates with reduced uncertainties. A refined model could prove helpful when chemical structures are tuned for better pharmacokinetic properties. Finally, our model for drug transport across the BBB, for general purpose, including the total concentration c_B of paclitaxel in the brain, is given by

$$\frac{dc_L}{dt} = \frac{2D_{LE}}{r_L}(c_{f,E} - c_{f,L}) + \frac{c_{f,E}}{K_M + c_{f,E}}\frac{J_{max}}{\pi r_L^2} \tag{17}$$

$$\frac{dc_E}{dt} = \frac{2r_L D_{LE}}{r_E^2 - r_L^2}(c_{f,L} - c_{f,E}) + \frac{2r_E D_{EB}}{r_E^2 - r_L^2}(c_{f,B} - c_{f,E}) - \frac{c_{f,E}}{K_M + c_{f,E}}\frac{J_{max}}{\pi(r_E^2 - r_L^2)} \tag{18}$$

$$\frac{dc_B}{dt} = \frac{2\pi}{V_B} r_E D_{EB} l \cdot (c_{f,E} - c_{f,B}) \tag{19}$$

with $l = 600$ km, $c_{f,B}$ being the free concentration of drug in the cerebro-spinal fluid, and V_B being the volume of this fluid. In the experiment with isolated brain capillaries, $c_{f,B}$ was the constant concentration of paclitaxel in the medium, c_M. We suggest $c_{f,E}$ and, depending on the application, $c_{f,L}$ to be calculated by equation (15), as a function of total concentration. The differential equation for each state, c_L, c_E and c_B, can be extended, e.g., c_L be linked to ADME (absorption, distribution, metabolism, excretion) kinetics of the drug.

Prima facie, blocking p-gp at the BBB with a selective inhibitor like valspodar seems to be the optimal solution for the paclitaxel-based chemotherapy of GBMs and other tumours of the CNS. However, complete inhibition of p-gp most probably would, due to the broad substrate specificity of p-gp, allow many other compounds enter the CNS, that would otherwise be excluded. This is nicely illustrated by the observation of opiate-like activity of the antidiarrheal drug loperamide in the CNS of p-gp knockout mice (Schinkel *et al.*, 1996). For that reason, more elaborate targeting techniques need to be developed. A promising approach is the use of paclitaxel-loaded liposomes that are coated with cationized albumin or with antibodies that specifically bind to proteins of the luminal surface of BCECs. Recently, it was shown that liposomes that are coated with cationized albumin are taken up by cultured BCECs and by intact brain capillaries, thus crossing the BBB (Thöle *et al.*, 2002). In general, targeted liposomes can be loaded not only with paclitaxel but with any other warhead against brain tumours, or even with any drug against CNS-related disease. For liposomes, the rate of drug release can be modulated by the lipid composition (Chang, 1994). While too high releasing rates yield empty liposomes at the BBB, too slow degradation of the liposomes or release of the drug in the endothelial cells would let the idea fail at saturating p-gp. Studying such scenarios is only one example for how the model presented here might support the rational development of technologies *in silico* for efficiently targeting the CNS across the BBB.

REFERENCES

Ball, E.G. and Cooper, O., 1952, The reaction of cytochrome oxidase with cyanide, *J Biol Chem*, 198: 629–638.

Bock, H.G., 1987, Randwertproblemmethoden zur Parameteridentifizierung in Systemen nichtlinearer Differentialgleichungen, in *Bonner Mathematische Schriften* (Vol. 3) (Universität Bonn, Bonn, Germany).

Caplow, M., Shanks, J. and Ruhlen, R., 1994, How Taxol modulates microtubule disassembly, *J Biol Chem*, 269: 23399–23402.

Chang, E.L., 1994, Unusual thermal stability of liposomes made from bipolar tetraether lipids, *Biochem Biophys Res Commun*, 202: 673–679.

Dermietzel, R., 1975, Junctions in the central nervous system of the cat. Part IV: Interendothelial junctions of cerebral blood vessels from selected areas of the brain, *Cell Tissue Res*, 164: 45–62.

Diehl, M., 2002, Real-time optimization for large scale nonlinear processes, in *Fortschr.-Ber. VDI Reihe 8, Meß-, Steuerungs- und Regelungstechnik*, (vol 920) (VDI Verlag, Düsseldorf, Germany). Available at: http://www.ub.uni-heidelberg.de/archiv/1659/.

Eisenblatter, T., Huwel, S. and Galla, H.J., 2003, Characterization of the brain multidrug resistance protein (BMDP/ABCG2/BCRP) expressed at the blood-brain barrier, *Brain Res*, 971: 221–231.

Fellner, S., Bauer, B., Miller, D.S., Schaffrik, M., Frankhänel, M., Spruß, T., Bernhardt, G., Graeff, C., Färber, L., Gschaidmeier, H., Buschauer, A. and Fricker, G., 2002, Transport of paclitaxel (taxol) across the blood-brain barrier in vitro and in vivo, *J Clin Invest,*, 110: 1309–1318.

Glantz, M.J., Chamberlain M.C., Chang, S.M., Prados, M.D. and Cole, B.F., 1999, The role of paclitaxel in the treatment of primary and metastatic brain tumours, *Semin Radiat Oncol*, 9: 27–33.

Heimans, J.J., Vermorken, J.B., Wolbers, J.G., Eeltink C.M., Meijer, O.W., Taphoorn, M.J. and Beijnen, J.H., 1994, Paclitaxel (taxol) concentrations in brain tumor tissue, *Ann Oncol*, 5: 951–953.

Henningsson, A., Karlsson, M.O., Viganò, L., Gianni, L., Verweij, J. and Sparreboom, A., 2001, Mechanism-based pharmacokinetic model for paclitaxel, *J Clin Oncol*, 19: 4065–4073.

Jang, S.H., Wientjes, M.G. and Au, J.L., 2001, Kinetics of p-glycoprotein-mediated efflux of paclitaxel, *J Pharmacol Exp Ther*, 298: 1236–1242.

Juliano, R.L. and Ling, V., 1976, A surface glycoprotein modulating drug permeability in Chinese hamster ovary cell mutants, *Biochim Biophys Acta*, 455: 152–162.

Kallrath, J., Bock, H.G. and Schlöder, J.P., 1993, Least squares parameter estimation in chaotic differential equations, *Celest Mech Dyn Astro*, 56: 353–371.

Leineweber, D.B., Schäfer, A., Bock, H.G. and Schlöder, J.P., 2003, An efficient multiple shooting based reduced SQP strategy for large-scale dynamic process optimization. Part II: Software aspects and applications, *Comp Chem Eng*, 27: 167–174.

Maggon, K., 2005, Best-selling human medicines 2002–2004, *Drug Discov Today*, 10: 739–742.

Martin, C., Berridge, G., Higgins C.F., Mistry, P., Charlton, P. and Callaghan, R., 2000, Communication between multiple drug binding sites on p-glycoprotein, *Mol Pharmacol*, 58: 624–632.

Melan, M.A., 1998, Use of fluorochrome-tagged taxol to produce fluorescent microtubules in solution, *Biotechniques*, 25: 188–192.

Rasband, W.S., 1997–2006, ImageJ, U. S. National Institutes of Health, Bethesda, Maryland, USA. Available at http://rsb.info.nih.gov/ij/.

Rowinsky, E.K., 1997, Paclitaxel pharmacology and other tumor types, *Semin Oncol*, 24: S19-1–12.

Schinkel, A.H., Wagenaar, E., Mol, C.A. and van Deemter, L., 1996, P-glycoprotein in the blood-brain barrier of mice influences the brain penetration and pharmacological activity of many drugs, *J Clin Invest*, 97: 2517–2524.

Seetharaman, S., Barrand, M.A., Maskell, L. and Scheper, R.J., 1998, Multidrug resistance-related transport proteins in isolated human brain microvessels and in cells cultured from these isolates, *J Neurochem*, 70: 1151–1159.

Steiner, H.H., Herold-Mende, C., Bonsanto, M., Geletneky, K. and Kunze, S., 1998, Prognosis of brain tumours: epidemiology, survival time, and clinical course, *Versicherungsmedizin*, 50: 173–179.

Thöle, M., Nobmann, S., Huwyler, J., Bartmann, A. and Fricker, G., 2002, Uptake of cationized albumin coupled liposomes by cultured porcine brain microvessel endothelial cells and intact brain capillaries, *J Drug Target*, 10: 337–344.

ACKNOWLEDGEMENT

The second author gratefully acknowledges support by the Research Council of K.U. Leuven funding the Optimization in Engineering Center OPTEC (CoE/EF/05/006) and by the Belgian Federal Science Policy Office within IUAP P6/04 (DYSCO: Dynamical systems, control and optimization, 2007–2011), as well as from the Interdisciplinary Center for Scientific Computing (IWR) of the University of Heidelberg.

The manuscript was received 7 December 2006 and accepted for publication after revision 23 April 2007.